2015 IEEE International Conference on Robotics and Automation (ICRA)
Washington State Convention Center
Seattle, Washington, May 26-30, 2015

Kinematic Analysis and Design Considerations for Optimal Base Frame Arrangement of Humanoid Shoulders

Mostafa Bagheri, Arash Ajoudani, Jinoh Lee, Darwin G. Caldwell and Nikos G. Tsagarakis

***Abstract*— It is well known that kinematics can significantly affect the manipulation capabilities of robotic arms, traditionally illustrated by performance indices such as workspace volume, kinematic and force manipulability, and isotropy within the arm workspace. In the case of dual-arm systems and bi-manual manipulation tasks, the kinematics effects to the above indices becomes even more apparent. However, in spite of the large number of dual-arm systems developed in the past, there is a little literature on the kinematic design analysis for the development of such systems. Particularly, the effects of configuration/orientation of the shoulders' placement with respect to the torso structure have not sufficiently studied or considered, while many dual-arm systems with upward and/or forward tilt angle in shoulder base frame have been introduced. This paper addresses this problem and quantifies the effect of shoulders base frame orientation in a dual-arm manipulation system by looking at its effect on several important manipulation indices, such as the overall and common workspace, redundancy, global isotropy, dual-arm manipulability, and inertia ellipsoid index within the common workspace of the two arms. Consequently, a range of upward and forward tilt angles for the shoulder frames is identified for the design of a dual-arm torso system to render the most desired manipulation performance.**

I. INTRODUCTION

The fast growing interest in dexterity and versatility of the manipulation skills has led to the development of several bi-manual robotic systems, ranging from a fixed base dual-arm station to mobile manipulation platforms mounted on a wheeled base, and eventually, humanoid robots [1]–[4]. These robots have offered the capability to perform coordinated bi-manual manipulation tasks in an attempt to effectively execute realistic tasks using tools designed for humans [5].

Traditional design of the dual-arm robots concerns the realization of an anthropomorphic structure with 7 degrees-of-freedom (DOFs) arms, three of which at the shoulder, one DOF at the elbow, and three DOFs at the forearm/wrist joints (examples include ARMAR [6], COMAN [7], [8], and HRP2 [9]). Even though these robots are potentially capable of demonstrating effective manipulation skills, the underlying concept of the arm design is only approximately equivalent for the human arm kinematic structure. This is due to the fact that humans have the ability to elevate (upward/downward) and to incline (forward/backward) the shoulder joints, utilizing supplementary kinematic redundancy of the arm to achieve a certain goal in task space (see example in Fig. 1). This additional mobility is usually coupled with shoulder motion and permits humans to extend their arm workspace and demonstrate broader manipulation capabilities.

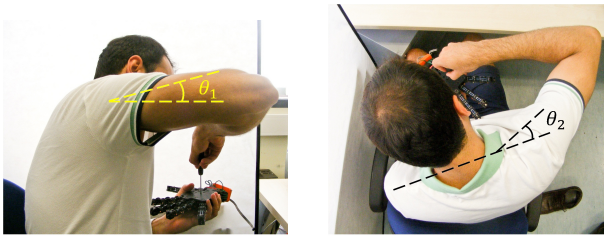

a) Upward/downward angle b) Forward/backward angle

Fig. 1. Scapula mobility of the human arm.

This implies that the kinematic structure of the humanoid shoulder may affect the single- and dual-arm manipulation capabilities by simply varying the upward and/or forward shoulder angles. Even if additional actuation mechanisms can be considered for the shoulder joints to further approximate the anthropomorphic structure, this will result in design complexity and control burden. Therefore, it is preferable that these angles are fixed. Such a consideration has been included in the design of a few robotic platforms, for examples, Justin robot [2], in which the arms are placed in a humanoid-like configuration with a tilt of 60 degrees, the Atlas robot [3], and ABB's Friendly Robot Industrial Dual-Arm (FRIDA) [10]. However, the effect of upward and forward angles has not been sufficiently studied or demonstrated.

In this paper, we study the effect of shoulders' base frame arrangement of the WALK-MAN robot[1] that will allow us to select an optimum range of upward and forward shoulder angles to achieve a desired manipulation performance. In this direction, important manipulation indices are introduced and evaluated in a prioritized order, which is achieved by taking into account the target tasks stated in [11], similar to the ones announced by the DARPA Robotics Challenge (DRC) [12]. For instance, considering the valve-turning and assembly tasks, the shared workspace realized by the two end-effectors, i.e. common workspace [13], [14], is defined as an important manipulation index [13]. Furthermore, in an attempt to effectively use the target tools (such as drill), other manipulation capabilities such as velocity and force manipulability [15], [16], range of swivel angle in the arms [17], dual-arm manipulability, global isotropy [16], and inertia ellipsoid [18] within the common workspace are taken into

The authors are with the Department of Advanced Robotics, Istituto Italiano di Tecnologia (IIT), Genoa, Italy mostafa.bagheri, arash.ajoudani, jinoh.lee, darwin.caldwell, nikos.tsagarakis@iit.it

[1]The humanoid robot is currently being designed within the EU project Whole-body Adaptive Locomotion and Manipulation, WALK-MAN [11].

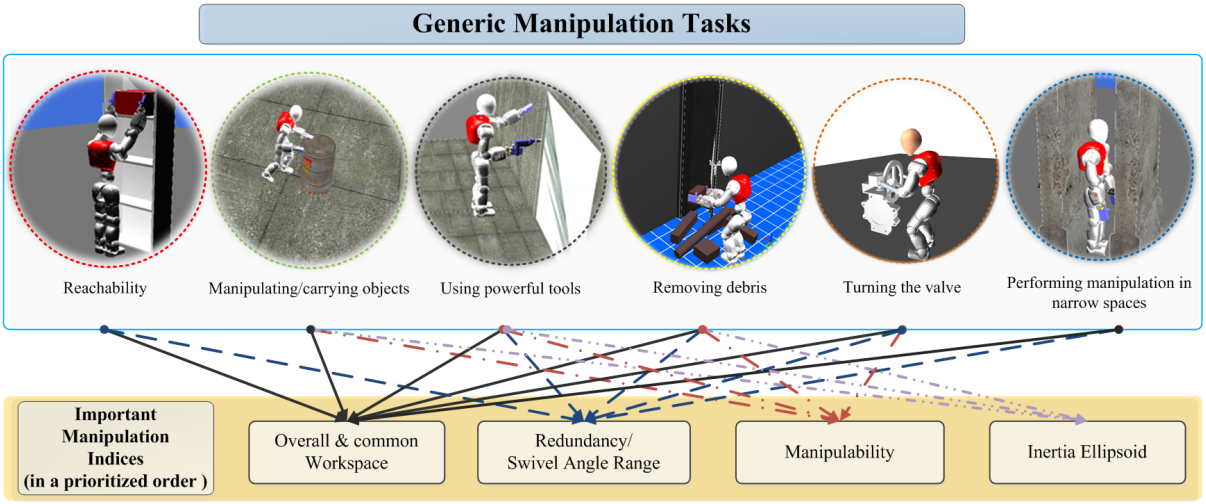

Fig. 2. Target bi-manual manipulation tasks used for the definition and prioritization of the performance indices.

account. Finally, following this analysis, we propose a range of upward and forward angles where the above-mentioned indices are optimized for the WALK-MAN humanoid robot in a predefined order of importance.

The rest of the paper is structured as follows. Section II introduces the manipulation performance indices. In section III, the effect of shoulder base frame arrangement in target manipulation indices is studied. Finally, Section IV addresses the conclusions.

II. Performance Indices

The WALK-MAN robot is being designed with two 7 DOFs redundant arms, 3 of which in the shoulder, 1 DOF in the elbow and 3 DOFs in the wrist joints, as shown in Fig. 3. The shoulder base frames are considered with two tilted angles: upward angle θ_1 and forward angle θ_2, resembling the rotation of the scapula of the human arm shown in Fig. 1.

To achieve an optimal manipulation performance in the WALK-MAN dual-arm system, a set of target manipulation tasks is taken into account (see Fig. 2), and the corresponding manipulability indices which contribute to the task execution performance are defined as

- the Product of Total and Common Workspace Area (PTCWA),
- Swivel Angle Range (SAR) within the common workspace which describes the redundancy range of the arms,
- the Global Isotropy Index (GII) for each arm within the common workspace which is a measure of the end-effector isotropy,
- Dual-arm Manipulability Index (DMI) within the common workspace, and
- the Global Inertia Ellipsoid Index (GIEI) within the common workspace which shows the inertial effect and nonlinearities of mechanical arms.

As mentioned before, the evaluation of the above indices is carried out in a prioritized order, taking into account the requirements of the target tasks. In each step, a desired range of the shoulder base frame angles which optimizes the corresponding index is calculated and used as an input range for the optimization of the lower-priority manipulation index. Eventually, last index will provide the desired range of the shoulder base frame tilt angles which optimize all the considered indices in a prioritized order.

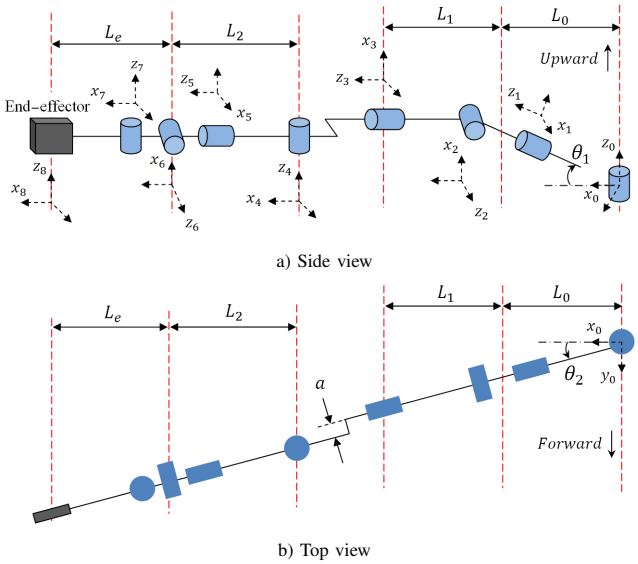

Fig. 3. Schematic diagram of the arm kinematics with two tilt angles, upward (θ_1) and forward (θ_2), in the shoulder joint.

A. Workspace Analysis

The Cartesian workspace represents the portion of the environment that the manipulator's end-effector can access. The shape and volume of the workspace depend on the manipulator kinematics as well as on the presence of mechanical joint limits, and it can be computed by considering the Direct Kinematics (DK) equation of the arm. To calculate the overall workspaces of the dual-arm system, the joint space of each arm is sampled and the end-effector position in the

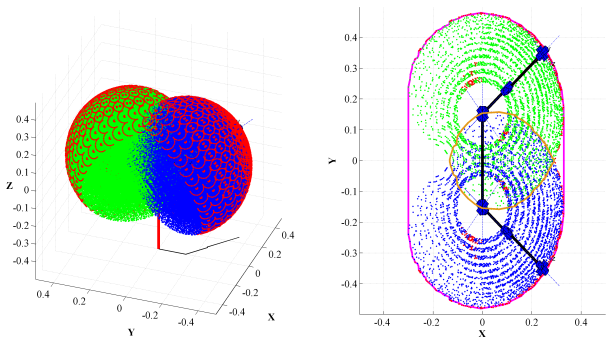

Fig. 4. a) Workspace and b) a cut through the total and common workspace of dual-arm robot in horizontal plane from top view.

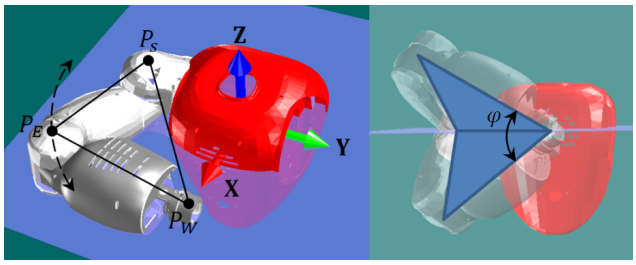

Fig. 5. Arm triangle and swivel angle range (φ) from front view of the robot.

Cartesian space is calculated using a random search approach [19]. Following that, an algorithm is implemented to account for the workspace of each arm and search for the shared volume between the right and the left arm workspaces which correspond to the common workspace area, in which bi-manual tasks can be effectively performed. Fig 4 illustrates the corresponding workspaces, coinciding with the torso x-y frame. The blue and green points correspond to the reachable points of the right and the left arm in space, respectively. The overall and common workspace boundaries are also plotted. The red points correspond the left/right arm singular configurations, and are excluded from the overall and common workspace areas. For this purpose, the manipulators' Jacobian determinant was used to determine whether or not a configuration is singular.

As the first priority for the optimization of upward and forward angles of the shoulder base frame, which contribute to the overall and common workspace areas, the Product of Total and Common Workspace Area (PTCWA) index is defined and calculated over the allowable range of shoulder base frame angles.

B. Swivel Angle

Arm redundancy, which occurs when the dimension of joint space is greater than that of the operational space required for the task execution, allows the optimal selection of joint configurations based on avoiding singularities as well as collisions and joint limits, balancing joint loads, minimizing the required energy or time, etc. Since the 7 DOFs arm model is redundant, the location and orientation of the hand does not fully specify the configuration of the arm. The configuration becomes fully defined when the elbow position (P_E) is specified. Obviously, the elbow position introduces three additional variables, but if the wrist position (P_W) is known, a single variable specifies the arm configuration. The arm forms a triangle with one corner point at the shoulder (P_S), one at the elbow and the third point at the wrist (Fig 5). Both the shoulder and wrist joints allow rotation of the elbow point around the vector starting from the shoulder and ending at the wrist ($\overrightarrow{P_S P_W}$) [20].

A local coordinate system gives a reference to measure the swivel angle (φ) of the elbow, so that it is zero when the elbow is in the minimum height (elbow down), and it is equal to the swivel angle rang, when the elbow is in the maximum height (elbow up). Fig. 5 illustrates the swivel angle rang for robot's arm, in reaching a certain point in common workspace. As the second performance index contributing to the dexterity of the manipulation, the arm redundancy range (swivel angle range) is defined here. Higher values of this index correspond to bigger range of arm motion which results in stronger manipulation capabilities. This is due to the fact that the stabilization of subtask variables using redundancy will be more feasible if this range is bigger.

To determine the arm redundancy range, the minimum height of the elbow is calculated by taking into account the constraints in the task (e.g. position of the wrist) and joint (e.g. joint limits) spaces using the following optimization law

$$\begin{aligned} &\min && \text{height of } P_E \text{ (Z coordinate of } P_E) \\ &\text{Subject to} && \left\{ \begin{array}{ll} P_W : \text{fixed} & \\ q_{im} \leq q_i \leq q_{iM} & i = 1, ..., n \end{array} \right\}, \end{aligned} \tag{1}$$

where q_{im} and q_{iM} denote the minimum and maximum limits at the joint i, respectively. Similarly, a similar optimization problem is utilized to account for the maximum height of elbow. Eventually, the range between the two extremes is calculated to describe the SAR index.

C. Dual-arm Manipulability and Global Isotropy

In the case of dual-arm cooperative task execution, the Dual-arm Manipulability (DM) is represented by the area of intersection between the two manipulability ellipsoids from individual arms as illustrated in Fig. 6. This implies that the required cooperation between the two arms imposes additional kinematic constraints on the manipulability of individual arms [15].

It is well known that more isotropic realization of the manipulability ellipsoid [2] and its higher volume results in a better velocity and force control in each direction in the workspace. To evaluate such a capability, the Globals Isotropy Index (GII) is defined by comparing the smallest and largest singular values of manipulability matrices in the entire common workspace [16]. This index assigns a value of

[2]The manipulability matrix $\mathbf{M} = \mathbf{J}\mathbf{J}^T$ is used to obtain the manipulability ellipsoid [21], which is defined for a given arm configuration and interpreted as a distance of the manipulator from a singular configuration.

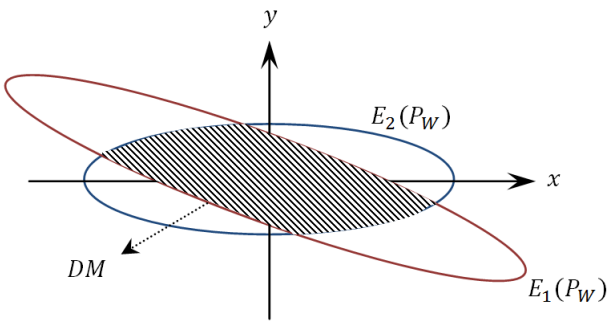

Fig. 6. Dual-arm manipulability.

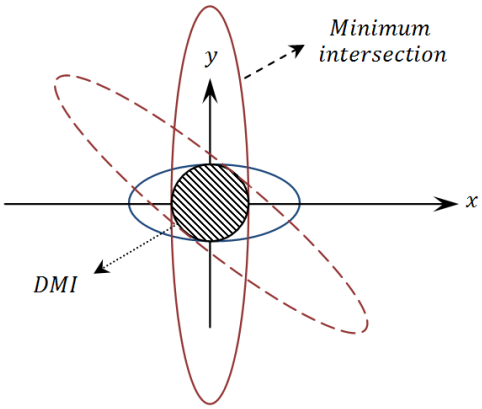

Fig. 7. Dual-arm manipulability in various configurations.

1 to the perfect isotropy and a value of 0 to singular behavior

$$\mathrm{GII} = \frac{\min\limits_{x_i \in W} \sigma_{min}(JJ^T)}{\max\limits_{x_i \in W} \sigma_{max}(JJ^T)} = \frac{\sigma_{min_G}}{\sigma_{max_G}}, \tag{2}$$

with W, J, σ_{min}, and σ_{max} representing the collection of the points (x_i) in the common workspace, the manipulator Jacobian, the minimum and maximum eigenvalues, respectively. $\sigma_{min_G}(\sigma_{max_G})$, the global minimum (maximum) eigenvalue, can be calculated using the following optimization law

$$\begin{aligned} &\min(\max) && \sigma(JJ^T) \\ &\text{Subject to} && \left\{ \begin{array}{c} P_W : \text{fixed} \\ q_{im} \le q_i \le q_{iM} \qquad i = 1, ..., n \\ |JJ^T| \ge 0.001 \end{array} \right\}, \end{aligned} \tag{3}$$

where $|.|$ symbolizes the determinant of the matrix. It is worth mentioning that finding the minimum isotropy within the workspace is equivalent to looking for the singular configurations, therefore, to perform a good comparison, it is necessary to consider a certain distance from the workspace points in which a singularity can occur. Moreover, it can be shown that the dual-arm's manipulability over the common workspace is always more than $\pi\sigma_{min_G}\sigma_{min_G}$. This condition happens when the two arms' manipulability ellipsoids are perpendicular, with both minimum eigenvalues equal to σ_{min_G} (see dashed area in Fig. 4). Therefore, the minimum DM within the common workspace for certain values of the shoulder tilt angles can be calculated by

$$\mathrm{DMI} = \pi(\sigma_{min_G})^2. \tag{4}$$

This index is called the Dual-arm Manipulability Index (DMI) and forms the forth priority performance index in our kinematic design.

D. Global Inertia Ellipsoid Index

The motion of a mechanical arm is highly nonlinear including Coriolis and centrifugal forces. These nonlinear forces are analyzed geometrically using the Inertia Ellipsoid (IE); so that if the IE is isotropic, those nonlinear forces do not appear [18]. The principal axes of the lE are aligned with the eigenvectors of the inertia matrix in Cartesian space, and the length of each principal axis is the reciprocal of the square root of the corresponding eigenvalue. Therefore, IE varies its configuration depending on the arm configuration.

In this section, the inertia ellipsoid, which is used for graphically representing the mass properties of a single rigid body, is extended to a Global Inertia Ellipsoid Index (GIEI) for a series of rigid bodies such as a robot arm, and utilized as one of performance indices in robot arm kinematic design. Therefore, GIEI is defined as the ratio of minimum over maximum axes values of the inertia ellipsoids as follows

$$\mathrm{GIEI} = \frac{\min \quad \sigma_{min}(J^{+T}\Lambda J^T)}{\max \quad \sigma_{max}(J^{+T}\Lambda J^T)}, \tag{5}$$

with J^+ denoting the generalized inverse of the Jacobian matrix and Λ is the arm's configuration dependent mass matrix, modeled by the ROBOTRAN simulator [22]. GIEI is defined to evaluate the effect of kinematic design in the dynamic manipulation capabilities of the WALK-MAN robot, so that the generalized moment of inertia is uniform in any direction over a wide range of common workspace.

III. Simulations and Results

As mentioned previously, the workspace of the dual-arm system is considered as the index with the highest priority. Therefore, the areas of the total and the common workspace of the two arms are calculated for the x-y plane of the torso frame, excluding the collision areas of the arms with the body (see Fig. 8).

The areas of total and common workspaces for θ_1 and θ_2 tilt angles are demonstrated in Fig. 9. This figure illustrates that the total workspace and the common workspace do not change significantly by increasing θ_1, while the effect of variation of θ_2 in the total and common workspace areas is major. Following that, the PTCWA index is calculated for the tilt angles within the range of 0 to 70 degrees for both θ_1 and θ_2 and demonstrated in Fig. 10.

Fig. 10 results suggest that the PTCWA is maximized when the forward angle (θ_2) varies within the range 40 to 70 degrees. Therefore, the following manipulation indices are evaluated within the reduced range ($40^o \le \theta_2 \le 70^o$) of the forward angle, while the whole range of θ_1 is explored.

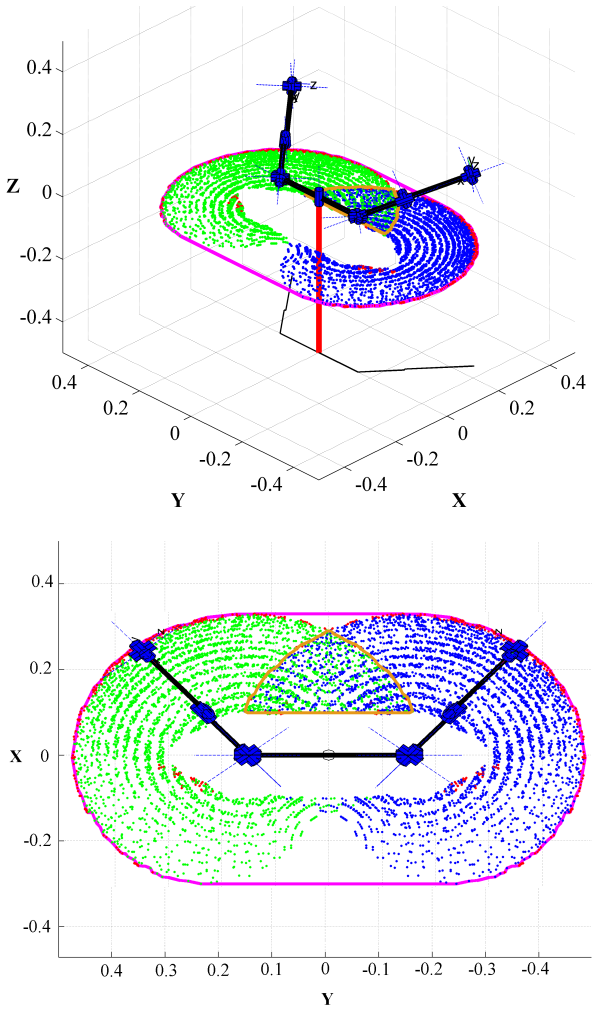

Fig. 8. The total and common workspace for the x-y plane of the torso.

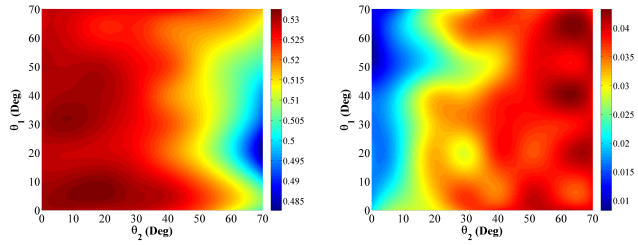

a) Total worksapce b) common worksapce

Fig. 9. a) Total workspace and b) common workspace in horizontal plane.

Following the workspace analysis, a range of tilt angles which contribute to a bigger redundancy range is identified. To achieve this, the SAR index is calculated within the previously defined tilt angle range for the all points in the common workspace area. As observed in Fig. 11, θ_1 variations efficiently affect the SAR index with the maximum values occurring in the range of $0^o \leq \theta_1 \leq 25^o$.

In addition to that, the ratio between the minimum and maximum SAR within the common workspace was calculated which is illustrated in Fig. 11 b. This ratio effectively

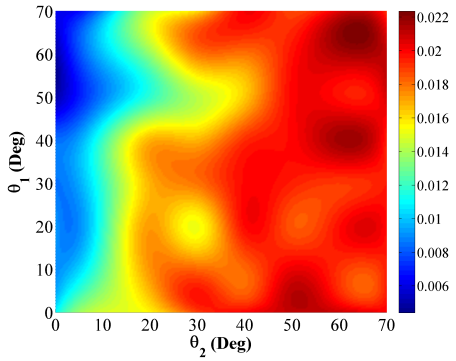

Fig. 10. PTCWA in horizontal plane.

demonstrates the isotropy of the SAR within the entire common workspace and indicates that the maximum redundancy range is achieved for shoulder base frame configurations $15^o \leq \theta_1 \leq 30^o$ and $45^o \leq \theta_2 \leq 65^o$.

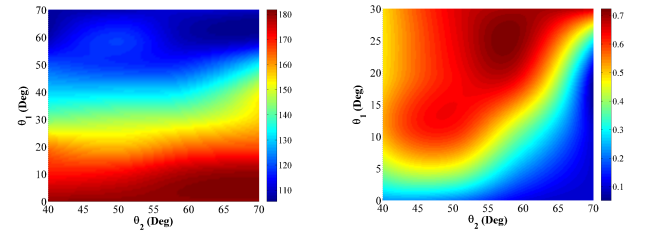

a) Maximum SAR in common workspace b) SAR ratio in common workspace

Fig. 11. SAR in common workspace.

Subsequently, the arms' GII and DMI are computed and compared for different shoulder base configuration, as demonstrated in Fig. 12, respectively. Maximized values of aforementioned indices occur when the shoulder tilt angles vary within $10^o \leq \theta_1 \leq 25^o$ and $55^o \leq \theta_2 \leq 65^o$.

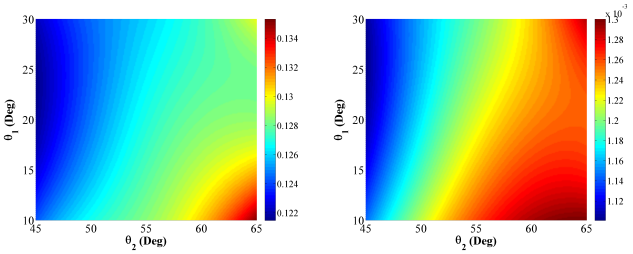

a) b)

Fig. 12. a) Arm's GII and b) minimum dual-arm manipulability.

Eventually, the mass properties and dynamic behavior of a robot manipulator is investigated by GIEI and demonstrated in Fig. 13. Maximized values for this index occur when the shoulder tilt angles vary within $20^o \leq \theta_1 \leq 30^o$ and $60^o \leq \theta_2 \leq 65^o$.

IV. Conclusions

This work introduces a procedure to optimize the kinematic placement of the shoulders of dual-arm manipulation

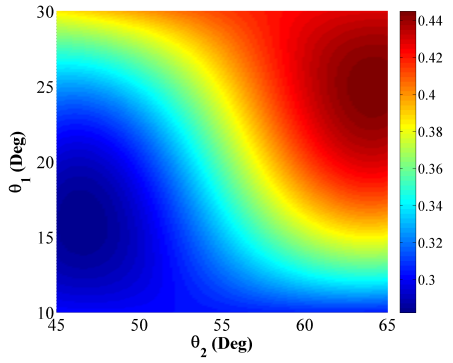

Fig. 13. Global inertia ellipsoid index.

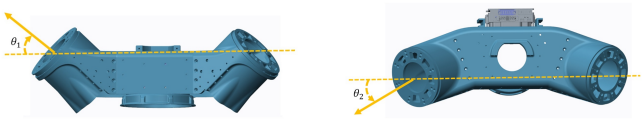

a) Upward angle b) Forward angle

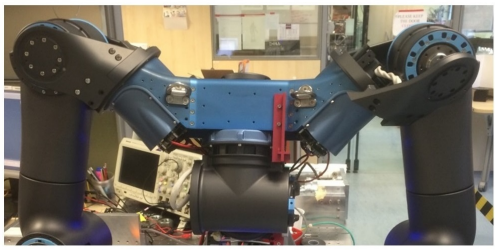

c) Front view of robot

Fig. 14. Shoulder base frame arrangement of the WALK-MAN robot.

systems with the aim to increase the manipulation capabilities of the dual-arm torso of the WALK-MAN humanoid robot. Based on this study the shoulder frame tilt angles were optimally identified. To achieve this, the Product of Total and Common Workspace Area (PTCWA), Swivel Angle Range (SAR), Global Isotropy Index (GII), Dual-arm Manipulability Index (DMI), and the Global Inertia Ellipsoid Index (GIEI) which contribute to the single- and dual-arm manipulation capabilities of the robot were defined and used for the optimization of the tilt angles in a prioritized order of importance.

The outcome of this study suggests that by taking into account the upward angle ($20^o \leq \theta_1 \leq 25^o$) and the forward angle ($60^o \leq \theta_2 \leq 65^o$) ranges in the kinematic design of the WALK-MAN robot, target tasks illustrated in [11] will be executed more effectively due to the increased single- and dual-arm manipulation capabilities. Figure 14 demonstrates the realized the shoulder base frame arrangement of the WALK-MAN humanoid robot.

V. Acknowledgments

This work is supported by the European Research Council under EU FP7-ICT project, WALK-MAN, "Whole-body Adaptive Locomotion and Manipulation", no. 611832.

References

[1] C. Smith, Y. Karayiannidis, L. Nalpantidis, X. Gratal, P. Qi, D. V. Dimarogonas, and D. Kragic, "Dual arm manipulationa survey," *Robotics and Autonomous Systems*, vol. 60, no. 10, pp. 1340–1353, 2012.

[2] C. Ott, O. Eiberger, W. Friedl, B. Bauml, U. Hillenbrand, C. Borst, A. Albu-Schaffer, B. Brunner, H. Hirschmuller, S. Kielhofer *et al.*, "A humanoid two-arm system for dexterous manipulation," in *Humanoid Robots, 2006 6th IEEE-RAS Int. Conf. on*. IEEE, 2006, pp. 276–283.

[3] E. Guizzo, "Darpa seeking to revolutionize robotic manipulation," *IEEE Spectr. Technol. Sci. News*, 2010.

[4] N. G. Tsagarakis, G. Metta, G. Sandini, D. Vernon, R. Beira, F. Becchi, L. Righetti, J. Santos-Victor, A. J. Ijspeert, M. C. Carrozza *et al.*, "icub: the design and realization of an open humanoid platform for cognitive and neuroscience research," *Advanced Robotics*, vol. 21, no. 10, pp. 1151–1175, 2007.

[5] J. Lee, A. Ajoudani, E. M. Hoffman, A. Rocchi, A. Settimi, M. Ferrati, A. Bicchi, N. G. Tsagarakis, and D. G. Caldwell, "Upper-body impedance control with variable stiffness for a door opening task," in *IEEE Humanoids 2014*, pp. 713–719.

[6] T. Asfour, K. Berns, and R. Dillmann, "The humanoid robot armar: Design and control," in *The 1st IEEE-ras int. conf. on humanoid robots (humanoids 2000)*. Citeseer, 2000, pp. 7–8.

[7] A. Ajoudani, J. Lee, A. Rocchi, M. Ferrati, E. M. Hoffman, A. Settimi, D. Caldwel, A. Bicchi, and N. Tsagarakis, "A manipulation framework for compliant humanoid coman: Application to a valve turning task," in *IEEE Int. Conf. on Humanoid Robots*, 2014, accepted.

[8] N. G. Tsagarakis, S. Morfey, G. M. Cerda, L. Zhibin, and D. G. Caldwell, "Compliant humanoid coman: Optimal joint stiffness tuning for modal frequency control," in *Robotics and Automation (ICRA), 2013 IEEE Int. Conf. on*. IEEE, 2013, pp. 673–678.

[9] S. Miossec, K. Yokoi, and A. Kheddar, "Development of a software for motion optimization of robots-application to the kick motion of the hrp-2 robot," in *Robotics and Biomimetics, 2006. ROBIO'06. IEEE Int. Conf. on*. IEEE, 2006, pp. 299–304.

[10] E. Guizzo and T. Deyle, "Robotics trends for 2012," *IEEE Robotics & Automation Magazine*, vol. 19, no. 1, pp. 119–123, 2012.

[11] WALK-MAN. (2013 - 2017) Whole-body adaptive locomotion and manipulation. European Community's 7th Framework Programme: FP7-ICT 611832. Cognitive Systems and Robotics: FP7-ICT-2013-10. [Online]. Available: http://www.walk-man.eu/

[12] E. Ackerman, "Darpa robotics challenge trials: What you should (and shouldn't) expect to see," *IEEE Spectrum*, vol. 19, 2013.

[13] H. M. Do, C. Park, and J. H. Kyung, "Dual arm robot for packaging and assembling of it products," in *Automation Science and Engineering (CASE), 2012 IEEE Int. Conf. on*. IEEE, 2012, pp. 1067–1070.

[14] J. Rastegar and B. Fardanesh, "Manipulation workspace analysis using the monte carlo method," *Mechanism and Machine Theory*, vol. 25, no. 2, pp. 233–239, 1990.

[15] S. Lee, "Dual redundant arm configuration optimization with task-oriented dual arm manipulability," *Robotics and Automation, IEEE Transactions on*, vol. 5, no. 1, pp. 78–97, 1989.

[16] L. Stocco, S. Salcudean, and F. Sassani, "Fast constrained global minimax optimization of robot parameters," *Robotica*, vol. 16, no. 06, pp. 595–605, 1998.

[17] C. A. Klein and B. E. Blaho, "Dexterity measures for the design and control of kinematically redundant manipulators," *The Int. Journal of Robotics Research*, vol. 6, no. 2, pp. 72–83, 1987.

[18] H. Asada, "Dynamic analysis and design of robot manipulators using inertia ellipsoids," in *Proceedings of 1984 IEEE International Conference on Robotics and Automation*. IEEE, 1984, pp. 94–102.

[19] D. Alciatore and C. Ng, "Determining manipulator workspace boundaries using the monte carlo method and least squares segmentation," *ASME Robotics: Kinematics, Dynamics and Controls*, vol. 72, pp. 141–146, 1994.

[20] N. I. Badler and D. Tolani, "Real-time inverse kinematics of the human arm," *Center for Human Modeling and Simulation*, p. 73, 1996.

[21] T. Yoshikawa, "Analysis and control of robot manipulators with redundancy," in *Robotics research: the first international symposium*. MIT press Cambridge, MA, 1984, pp. 735–747.

[22] P. Fisette and J. Samin, "Robotran: Symbolic generation of multi-body system dynamic equations," in *Advanced Multibody System Dynamics*. Springer, 1993, pp. 373–378.